

Migration Law of Atrazine During Freezing of Water

Yan Zhang (✉ zhangyanytu@ytu.edu.cn)

Yantai University

Wanli Zhao

Yantai University

Aixin Yu

Yantai University

Yucan Liu

Yantai University

Fangyun Ren

Yantai University

Tongguo Zhao

Yantai University

Tongshuai Liu

Yantai University

Research Article

Keywords: atrazine, simulated freezing, migration law, distribution coefficient (K)

Posted Date: September 21st, 2021

DOI: <https://doi.org/10.21203/rs.3.rs-805749/v1>

License: © ⓘ This work is licensed under a Creative Commons Attribution 4.0 International License.

[Read Full License](#)

Abstract

To explore the migration law of atrazine during the freezing process, an indoor simulated freezing experiment was carried out. The distribution coefficient (K) was used to characterize the migration ability of atrazine and explore the effects of freezing thickness, freezing temperature, and initial concentration on the migration of atrazine between ice and water. The research results showed that the concentration relationship between the ice and water phases was: ice < water before freezing < water under the ice. This indicates that atrazine migrated to the water under the ice during the freezing process in our experiment. The K value decreased as the ice thickness, freezing temperature, and initial concentration increased; thus, the greater the ice thickness, the higher the freezing temperature, the greater the initial atrazine concentration, and the greater the ability of atrazine to migrate to the water under the ice. This study provides a reference for managing natural waterbodies in high-latitude and high-altitude environments during the freezing period.

1 Introduction

Freezing is an important hydrological feature of water bodies in high-altitude and high-latitude regions [1], with more than 50 million lakes in the world freezing regularly [2]. The existence of an ice sheet affects the light transmittance, and reduces the material and energy exchange rates between the atmosphere and a waterbody [3]. Moreover, it also reduces the rate of various biochemical reactions [4, 5] and hinders a waterbody's reoxygenation process [6–8], dilution process [9], and photolysis reaction [10], thereby greatly weakening the self-purification capacity of a waterbody under ice [11, 12].

Among the published literature on freshwater research, only 2% of the studies have considered the freezing process of waterbodies [10]; the primary focus has been on research related to conventional pollutants such as nitrogen, phosphorus, and metal ions. For example, Hampton et al. [10] conducted the first global quantitative integration of 101 lakes, and found that the total dissolved nitrogen and total nitrogen in these waterbodies during the freezing period were higher. Claude et al. [4] studied dissolved colored organic matter in polar regions and mountain lakes, and only found a relatively small concentration of low molecular weight pollutants in ice bodies, with most of the pollutants having been discharged into waterbodies. Powers et al. [5] determined that the nitrate-nitrogen concentration of a lake continued to increase during the freezing period, and observed a strong positive correlation between the number of frozen days in the lake. Xue et al. [13] studied the distribution of haloacetic acid precursors in a water–ice system during the freezing of water. Gao et al. [14–16] explored the effects of the freezing process on various organic pollutants in wastewater and wastewater toxicity. Li et al. [17] studied the migration of nitrobenzene between ice and water through an indoor simulation of the natural freezing process of rivers. Finally, Gao et al. [18] studied the distribution of *m*-cresol in the ice phase through indoor simulation experiments. Despite this research, studies regarding the pollution characteristics of persistent organic pollutants such as atrazine in waterbodies during the freezing period are still scarce.

Atrazine is one of the most widely used herbicides [19]. It has a high detection rate in natural water because it is widely used, stable chemical properties, strong water solubility, and recalcitrance to biodegradation [20]. Hence, atrazine poses a threat to the ecological environment and compromises the safety of drinking water [21]. Although considerable research progress has been made with respect to the pollution characteristics of atrazine during the nonfreezing period of waterbodies [22, 23], information is still lacking for the freezing period. Accordingly, this study performed an indoor simulation of the natural freezing process to explore the migration law of atrazine during the freezing process. The influences of freezing thickness, freezing temperature, and initial concentration on the migration law of atrazine are investigated. The results obtained herein can provide the basis for managing of natural waterbodies in high-altitude and high-latitude environments during the freezing period.

2. Materials And Methods

2.1 Experimental setup

In order to simulate the top-down freezing process of natural waterbodies, this study used a self-made, one-way unidirectional cold freezing simulation device (Fig. 1, left). The water sample was placed in a cylindrical glass container (diameter 10 cm and height 29.5 cm). The circumference and bottom of the glass container were then wrapped with polystyrene (EPS) insulation material to block the heat transfer between the barrel and the outside. The experimental device was placed in a low-temperature experiment box with temperature control. The temperature difference between the experimental box and the specified temperature did not exceed 0.5°C to ensure that the ice body gradually grew from top to bottom. The obtained ice sample was melted in an ice melting device with a cylindrical glass wall (Fig. 1, right), and the ice-melt water was collected.

2.2 Instruments and reagents

Main testing instruments: Ultra-high-performance liquid-chromatography electrospray triple-quadrupole mass spectrometer (UPLC–MS/MS) and an ACQUITY™ UPLC BEN C8 chromatographic column (2.1 mm × 50 mm × 1.7 μm).

Main reagents: Atrazine standard product (purity of > 98.8%), methanol (HPLC grade chromatographic purity of > 99.9%), and ultrapure water.

2.3 UPLC method parameters

Chromatographic conditions: The mobile phase was methanol (A) and 0.1% formic acid in water (B). The flow rate was set to 5.0 μL·min⁻¹ and 0.2 mL·min⁻¹. The column temperature was 35°C and the room temperature for sampling was 15°C. The injection volume was 5 μL.

Mass spectrometry conditions: Electrospray ion source (ESI) as positive ion mode acquisition; multiple reaction monitoring (MRM) mode. The capillary voltage and cone voltage were 3.3 kV and 35 V, respectively. The ion source temperature and desolvation (nitrogen) temperature were 120°C and 350°C,

respectively. The desolvation flow rate and the cone (nitrogen) flow rate were $500 \text{ L}\cdot\text{h}^{-1}$ and $30 \text{ L}\cdot\text{h}^{-1}$, respectively. The MRM parameters are listed in Table 1.

Table 1
MRM method parameters of atrazine

Compound	Mass to charge ratio m/z		Collision energy /eV
	Parent ion	Daughter ion	
Atrazine	215	95.8	25
		103.73	28
		173.9	17

2.4 Method precision

In the concentration range of $0\text{--}100 \mu\text{g}\cdot\text{L}^{-1}$, this method exhibited a good linearity for detecting atrazine ($Y = 1337.6X + 6314.4$; $R^2 = 0.995$). At the three concentrations of $5 \mu\text{g}\cdot\text{L}^{-1}$, $25 \mu\text{g}\cdot\text{L}^{-1}$, and $45 \mu\text{g}\cdot\text{L}^{-1}$ corresponding to low, medium, and high, the recovery rate of the standard addition was between 96% and 112%, and the relative standard deviation (RSD) of the determination was between 0.39% and 0.92%. Hence, the method was accurate and reliable.

2.5 Experimental design

In order to study the migration law of atrazine during the freezing process, and the influence of freezing thickness, freezing temperature, and initial concentration on the migration law, the following three experiments were designed.

(1) To explore the influence of freezing thickness on the migration of atrazine, 7.2 L of atrazine solution with an initial concentration of $15 \mu\text{g}\cdot\text{L}^{-1}$ was prepared. It was then divided into four parts which were equal in volume and poured into four freezing simulators, which were placed in low-temperature boxes at -5°C . When the ice thickness reached 3 cm, 6 cm, 9 cm, and 12 cm, ice samples and water samples from under the ice were collected. Each ice sample was layered every 3 cm from top to bottom, and the samples were labeled as ice 1, ice 2, ice 3, and ice 4. Samples were then analyzed after melting at room temperature (22°C).

(2) In order to explore the influence of freezing temperature on the migration of atrazine, 5.4 L of atrazine solution with an initial concentration of $15 \mu\text{g}\cdot\text{L}^{-1}$ was prepared. It was then divided into three parts which were equal in volume and poured into three freezing simulators, which were placed in low-temperature boxes at -5°C , -10°C , and -15°C . When the ice thickness reached 9 cm, ice samples and water samples from under the ice were collected following the procedure above. Samples were analyzed after melting at room temperature.

(3) In order to explore the influence of initial concentration on the migration law of atrazine, 1.8 L of atrazine solution was prepared at five different concentrations ($5 \mu\text{g}\cdot\text{L}^{-1}$, $15 \mu\text{g}\cdot\text{L}^{-1}$, $25 \mu\text{g}\cdot\text{L}^{-1}$, $35 \mu\text{g}\cdot\text{L}^{-1}$, $45 \mu\text{g}\cdot\text{L}^{-1}$). Each one was poured into a freezing simulator, which was placed in a low-temperature box at -10°C . When the ice thickness reached 9 cm, ice samples and water samples were collected from under the ice following the procedure above. Samples were analyzed after melting at room temperature.

2.6 Analysis method

The distribution coefficient (K) was used to express the migration ability of atrazine during freezing, as defined by Eq. (1):

$$K = \frac{C_i}{C_w}$$

1

where C_i is the atrazine concentration of melted water and C_w is the atrazine concentration of water under ice. The lower the K value, the stronger the ability of atrazine to migrate to water under ice.

3 Results And Analysis

3.1. Migration of atrazine between ice and water during freezing

Use the change of atrazine concentration to show the migration of atrazine in ice and water. As shown in Figure 2(a), when the ice thickness reached 3 cm, 6 cm, 9 cm, and 12 cm, the atrazine concentration of the i) ice-melt water was $0.55 \mu\text{g}\cdot\text{L}^{-1}$, $0.19 \mu\text{g}\cdot\text{L}^{-1}$, $0.22 \mu\text{g}\cdot\text{L}^{-1}$, and $0.22 \mu\text{g}\cdot\text{L}^{-1}$, and ii) water under the ice was $16.93 \mu\text{g}\cdot\text{L}^{-1}$, $19.63 \mu\text{g}\cdot\text{L}^{-1}$, $23.32 \mu\text{g}\cdot\text{L}^{-1}$, and $28.58 \mu\text{g}\cdot\text{L}^{-1}$ (i.e., increased from $15 \mu\text{g}\cdot\text{L}^{-1}$). This means that the atrazine concentration of the water under the ice increased with an increased ice thickness.

As shown in Figure 2(b), when the freezing temperature was -5°C , -10°C , and -15°C , the atrazine concentration of the i) ice-melt water was $0.22 \mu\text{g}\cdot\text{L}^{-1}$, $0.39 \mu\text{g}\cdot\text{L}^{-1}$, and $0.70 \mu\text{g}\cdot\text{L}^{-1}$, and ii) the water under the ice was $23.32 \mu\text{g}\cdot\text{L}^{-1}$, $23.19 \mu\text{g}\cdot\text{L}^{-1}$, and $23.03 \mu\text{g}\cdot\text{L}^{-1}$ (i.e., increased from $15 \mu\text{g}\cdot\text{L}^{-1}$). These results indicate that the atrazine concentration of the water under the ice decreased as the freezing temperature decreased; the lower the freezing temperature was, the more atrazine remained in the ice.

As shown in Figure 2(c), when the ice thickness was 9 cm, the atrazine concentration of the i) ice-melt water obtained at different initial atrazine concentrations was $0.23 \mu\text{g}\cdot\text{L}^{-1}$, $0.22 \mu\text{g}\cdot\text{L}^{-1}$, $0.33 \mu\text{g}\cdot\text{L}^{-1}$, $0.40 \mu\text{g}\cdot\text{L}^{-1}$, $0.45 \mu\text{g}\cdot\text{L}^{-1}$, and ii) the atrazine concentration increased from $5 \mu\text{g}\cdot\text{L}^{-1}$, $15 \mu\text{g}\cdot\text{L}^{-1}$, $25 \mu\text{g}\cdot\text{L}^{-1}$, $35 \mu\text{g}\cdot\text{L}^{-1}$, $45 \mu\text{g}\cdot\text{L}^{-1}$ before freezing to $7.69 \mu\text{g}\cdot\text{L}^{-1}$, $23.32 \mu\text{g}\cdot\text{L}^{-1}$, $38.99 \mu\text{g}\cdot\text{L}^{-1}$, $54.28 \mu\text{g}\cdot\text{L}^{-1}$, and $69.98 \mu\text{g}\cdot\text{L}^{-1}$ in the

water under the ice; hence, the atrazine concentration of the ice-melt water increased with an increase in the initial atrazine concentration.

Under the conditions of different ice thicknesses, freezing temperatures, and initial atrazine concentrations of the solution, the concentration relationship of atrazine in each phase was as follows: concentration in ice-melt water < initial concentration of water before freezing < concentration of the water under the ice. The atrazine concentration of the ice was smaller than that of the water before freezing, while the atrazine concentration of the water under the ice was higher. This indicates that atrazine migrated from the ice to the water under the ice during the freezing process.

3.2. Migration ability of atrazine under different factors

The migration ability of atrazine under different influencing factors is reflected in the change in the K value. As shown in Figure 2(a), when the ice thickness was 3 cm, 6 cm, 9 cm, and 12 cm, the K value was 0.0311, 0.0134, 0.0085, and 0.0047, respectively. As the ice thickness increased, the K value exhibited an increasing trend. Hence, the ability of atrazine to migrate from the ice to the water was enhanced as the ice thickness increased. As shown in Figure 2(b), when the freezing temperature was $-5\text{ }^{\circ}\text{C}$, $-10\text{ }^{\circ}\text{C}$, and $-15\text{ }^{\circ}\text{C}$, the K value was 0.01, 0.02, and 0.03, respectively; hence, the K value presented an increasing trend. Thus, the ability of atrazine to migrate from the ice to the water decreased as the freezing temperature decreased. As shown in Figure 2(c), when the initial atrazine concentration of the solution was $5\text{ }\mu\text{g}\cdot\text{L}^{-1}$, $15\text{ }\mu\text{g}\cdot\text{L}^{-1}$, $25\text{ }\mu\text{g}\cdot\text{L}^{-1}$, $35\text{ }\mu\text{g}\cdot\text{L}^{-1}$ and $45\text{ }\mu\text{g}\cdot\text{L}^{-1}$, the K value was 0.03, 0.009, 0.008, 0.007, and 0.006, respectively. Therefore, the ability of atrazine to migrate from the ice to the water increased as the initial atrazine concentration of the solution increased. In summary, the K value decreased with an increased freezing temperature, freezing thickness, and initial concentration. This demonstrates that the migration ability of atrazine was positively correlated with freezing thickness, freezing temperature, and initial concentration. Hence, increased freezing temperature, freezing thickness, and initial concentration are conducive to the migration of atrazine from ice to water under ice.

4 Discussion

4.1 Migration mechanism of atrazine between ice and water during freezing

The migration process of atrazine between ice and water could be explained by the formation and growth of ice. After placing the freezing container in the low-temperature experiment box, the temperature of the solution surface was first reduced. When it reached $0\text{ }^{\circ}\text{C}$, surface water molecules formed small, flat ice crystals under the action of hydrogen bonding. As the growth rate of ice crystals exceeded the nucleation rate, atrazine molecules were repelled to the ice–water interface, thus making the atrazine concentration at the ice–water interface much higher than that in the water under the ice. Driven by the concentration difference, atrazine at the ice–water interface diffused into the water under the ice. At the same time,

almost pure water molecules in the aqueous solution under the ice continued to migrate to the ice–water interface and froze on the lower surface of the ice layer [24]. In addition, as the temperature and energy of the ice–water system decreased, the solvation of atrazine by water molecules weakened, it can be imagined that the atrazine molecules were “squeezed out” of the ice phase to allow them to migrate into the water under the ice [25]; thus, the atrazine concentration of the water under the ice continued to increase.

However, not all of the atrazine was excluded into the water under the ice, and the discharge capacity of the ice was limited during the growth process of the ice; hence, some of the atrazine was retained within the ice. Especially during the early stage of freezing, water was in direct contact with the cold source and the freezing rate was higher. The dendritic ice crystals that were produced for a faster heat dissipation increased the adsorption of atrazine [26]. The adsorption process of atrazine molecules was similar to the capture process of salt packets during seawater freezing [27], and a small number of atrazine molecules froze in the ice before they could be squeezed out. In addition, a branching migration channel formed in ice during the freezing process, and atrazine trapped in the ice under the action of gravity migrated downwards through the channel. However, as the ice thickness increased, the ice growth rate slowed and the pore channel density decreased [28]. The undischarged atrazine froze in the lower pore channels; thus, it was difficult for it to further migrate to the water under the ice, thereby finally forming the ice structure shown in Figure 3.

The migration process of atrazine between ice and water can be verified by the theory of mass conservation. During the freezing process, as the volume of ice gradually increased, the volume of water under the ice decreased ($dV_w < 0$), and the atrazine concentration of water under the ice increased ($dC_w > 0$). According to the mass balance of atrazine in the ice–water phases, Equation (2) can be derived [29]:

$$C_w V_w = C_i dV_w + (C_w + dC_w)(V_w + dV_w) \quad (2)$$

According to Equations (1) and (2), Equations (3) and (4) can be derived:

$$\frac{dC_w}{C_w} = (1 - K) \frac{dV_w}{V_w} \quad (3)$$

The $-(dC_w dV_w)/(C_w V_w)$ term in the equation was ignored because it was small. By integrating both sides of Equation (3), it can be converted into the relationship between the volume ratio relative to the initial volume (V_w/V_0) and the concentration ratio relative to the initial concentration (C_w/C_0):

$$\ln\left(\frac{C_w}{C_0}\right) = (1 - K) \ln\frac{V_w}{V_0} \quad (4)$$

where C_0 is the initial concentration of atrazine before freezing and V_0 is the initial volume of atrazine before freezing. Figure 4 shows the linear plot of the K value for a 1.8 L water sample with an initial concentration of $15 \mu\text{g}\cdot\text{L}^{-1}$, which was frozen at $-5 \text{ }^\circ\text{C}$ to a 12 cm ice thickness. The atrazine concentration of the water under the ice was $28.58 \mu\text{g}\cdot\text{L}^{-1}$ and the volume of water under the ice was 0.936 L. According to Equation (4), the K value was calculated to be 0.0046, the correlation coefficient was 0.99995, and the error from the actual K value of 0.0042 at a 12 cm ice thickness was $< 10\%$. This model used the theory of mass conservation to explain the migration of atrazine.

4.2 Influence of various factors on the migration capacity of atrazine

The migration ability of atrazine in ice–water phases is affected by factors including ice thickness, freezing temperature, and initial concentration. During the freezing process, as temperature decreases, ice crystals gradually grow and form ice caps. The presence of ice caps weakens the heat exchange between the solution and surface gas. With the continuous increase in ice thickness, the growth rate of ice decreases, and the ice body has a better effect on removing discrete ice. In this study, the ability of the ice body to capture atrazine was weakened, which reduced the atrazine concentration of the ice [30, 31] and enhanced the ability of atrazine to migrate from the ice to the water under the ice.

The freezing temperature determines the freezing rate, nuclear density, shape, and size of ice crystals. As the freezing temperature decreases, more crystal nuclei and ice crystal branches are produced in the ice body, the freezing rate of ice increases, and the water molecules move to the ice–water interface faster. Once this speed exceeds the speed of atrazine moving to the interface, atrazine will be trapped by ice [32, 33]. At the same time, as the freezing temperature reduces, the solution area for the release latent heat increases and ice crystals grow in dendrites. In addition, more branches are produced on the trunk, and atrazine is more likely to be "trapped" by dendritic ice crystals or branch gaps. The purity of ice crystals then decreases and the K value increases with decreasing temperature [34–36]; hence, the migration ability of atrazine from ice to water under ice is weakened. For atrazine solutions with different initial concentrations, the freezing point decreases as the initial concentration of the solution increases. The stability of the ice–water interface also decreases and the formation of dendritic ice crystals with higher branches can capture atrazine more easily, thus reducing the purity of ice crystals [37]. On the other hand, an increased initial concentration of the solution also increases the number of potential crystal nuclei in the solution. Moreover, the frequency and energy of collisions between crystal nuclei increase, the probability of secondary nucleation increases, ice crystal growth accelerates, and purity decreases [38]. The atrazine concentration in ice increases as the solution concentration increases [39]. However, although the amount of captured atrazine in ice increases, it is more advantageous for atrazine to migrate to water under ice during the freezing process, the increase in atrazine concentration in ice at various concentrations was less than the migration [40]. Therefore, the K value of atrazine decreases with

an increase in the initial concentration, and the migration ability of atrazine from ice to water under ice increases.

5 Conclusion

(1) The concentration relationship of atrazine in ice–water phases under various influencing factors was: ice < water before freezing < water under ice. In our experiments, atrazine continuously migrated from the ice to the water under the ice during the freezing process. The migration ability of atrazine was positively correlated with freezing thickness, freezing temperature, and initial concentration. The K value decreased with increasing freezing temperature, freezing thickness, initial concentration; thus, we infer that these factors are beneficial to the migration of atrazine to water under ice.

(2) As atrazine migrates to water under ice during the freezing process, this may increase the ecological risk posed by atrazine to subglacial waters. Therefore, it is necessary to focus on water quality changes in subglacial waters of high-altitude and high-latitude regions during the freezing period.

(3) In addition to the factors investigated in this study, there may be many other factors affecting the migration of atrazine during the water freezing process, for example, pH and dissolved oxygen, which need to be further explored.

Declarations

Acknowledgments

This work was supported by the National Natural Science Foundation of China (No.51609207), the Foundation for Outstanding Young Scientist in Shandong Province (No.BS2014HZ021) and Shandong Provincial Natural Science Foundation of China (ZR2017BEE016).

References

1. Weyhenmeyer, G. A. *et al.* Large geographical differences in the sensitivity of ice-covered lakes and rivers in the Northern Hemisphere to temperature changes[J]. *Glob. Change Biol*, **17** (1), 268–275 (2015).
2. Verpoorter, C. *et al.* A global inventory of lakes based on high-resolution satellite imagery[J]. *Geophys. Res. Lett*, **41**, 6396–6402 (2014).
3. Fang, X. & Stefan, H. G. Simulations of climate effects on water temperature, dissolved oxygen, and ice and snow covers in lakes of the contiguous U.S. under past and future climate scenarios[J]. *Limnology & Oceanography*, 2009, 54(6, part, 2): 2359–2370.
4. Claude, B., John, A. E. G. & Warwick, F. V. *Colored dissolved organic matter and dissolved organic carbon exclusion from lake ice: Implications for irradiance transmission and carbon cycling*[J]

- 471283–1293(Limnology & Oceanography, 2002). 5
5. Powers, S. M. *et al.* Ice duration drives winter nitrate accumulation in north temperate lakes[J]. *Limnology & Oceanography Letters*, **2** (5), 177–186 (2017).
 6. Golosov, S. *et al.* Physical Background of the Development of Oxygen Depletion in Ice-Covered Lakes[J]., **151** (2), 331–340 (2007).
 7. Julie, T., Amir, S. & Karl-Erich, L. Modelling Dissolved Oxygen/Sediment Oxygen Demand under Ice in a Shallow Eutrophic Prairie Reservoir[J]., **9** (2), 131 (2017).
 8. Hampton, S. E. *et al.* Ecology under lake ice[J]. *Ecol. Lett*, **20**, 98–111 (2017).
 9. Zhang, Y. *Migration mechanism of pollutants and its application in ulansuhai lake in freezing process [D]* (Inner Mongolia Agricultural University, 2012).
 10. Hampton, S. E. *et al.* Heating up a cold subject: prospects for under-ice plankton research in lakes[J]. *Journal of Plankton Research*, **37** (2), 277–284 (2015).
 11. Huang, W. *et al.* Field observations on water temperature and stratification in a seasonally ice-covered shallow thermokarst lake[J]. *Advances in Water Science*, **27** (02), 280–289 (2016).
 12. Wang, Y. *et al.* Effect of simulated warming on microbial community in glacier forefield[J]. *Environmental Science*, **41** (06), 2918–2923 (2020).
 13. Xue, S. *et al.* Ratio of haloacetic acids precursor in water-ice system during the freezing processes of water[J]. *China Environmental Science*, **34** (11), 2773–2780 (2014).
 14. Gao, W., Smith, D. W. & Seago, D. C. Treatment of pulp mill and oil sands industrial wastewaters by the partial spray freezing process[J]. *Water Res*, **38** (3), 579–584 (2004).
 15. Gao, W., Smith, D. W. & Habib, M. Petroleum refinery secondary effluent polishing using freezing processes-toxicity and organic contaminant removal[J]. *Water Environ. Res*, **80** (6), 517–523 (2008).
 16. Gao, W. & Shao, Y. Freeze concentration for removal of pharmaceutically active compounds in water[J]., **249** (1), 398–402 (2009).
 17. Li, Z. *et al.* Distribution of nitrobenzene in water-ice system under different conditions[J]. *Science in China (Series E: Technical Science)*, **38** (07), 1131–1138 (2008).
 18. Gao, H. *et al.* Laboratory Study on the Distribution and Release Law of 3-methyl phenol in Ice[J]. *Science Technology and Engineering*, **8** (10), 2732–2735 (2008).
 19. Liu, Y. *et al.* *Degradation effect and mechanism of atrazine in UV-based oxidation processes[J]* 3560–66(China Water & Wastewater, 2019). 5
 20. Ouyang, W. *et al.* Occurrence, transportation, and distribution difference of typical herbicides from estuary to bay[J].Environment International, 2019,130,104858.
 21. Yang, L. *et al.* Environmental risk assessment of triazine herbicides in the Bohai Sea and the Yellow Sea and their toxicity to phytoplankton at environmental concentrations.Environment International, 2019,133,105175.
 22. Ouyang, W. *et al.* Typical pesticides diffuse loading and degradation pattern differences under the impacts of climate and land-use variations[J]. Environment International, 2020, 139,105717.

23. Xu, C. *Occurrence characteristics and transport modeling of trace organic contaminants in typical estuary reservoirs[D]* (Shanghai Jiao Tong University, 2018).
24. Lv, H. *et al.* Pollutant distribution under different conditions in Lake Ulansuhai ice-water system[J]. *Journal of Lake Sciences*, **27** (6), 1151–1158 (2015).
25. Zhang, Y. *et al.* Analysis on polluting characteristics in Hulun Lake during ice-on period and its application in field of water treatment[J]. *Ecology and Environmental Sciences*, **20** (2), 1289–1294 (2011).
26. Nakawo, M. Growth Rate and Salinity Profile of First-Year Sea Ice in the High Arctic[J]. *Research of Environmental Science*, 1981, 27(96):315–330.
27. Weeks, W. F. & Ackley, S. F. The growth, structure and properties of sea ice[J]. *The Geophysics of sea ice*, 1989:9–164.
28. Martin, S. A field study of brine drainage and oil entrainment in first-year sea ice[J]. *Journal of Glaciology*, **22** (88), 473–502 (1979).
29. Fujioka, R. *et al.* Application of progressive freeze-concentration for desalination[J]., **319**, 33–37 (2013).
30. Xue, S., Chen, J. & Tie, M. Release of dissolved organic matter from melting ice[J]. *Environmental Progress & Sustainable Energy*, 2016, 35(5):1458–1467.
31. Belen, F. *et al.* One option for the management of wastewater from tofu production: Freeze concentration in a falling-film system[J]. *Journal of Food Engineering*, **110** (3), 364–373 (2012).
32. Wharton, R. A. *et al.* Perennial ice covers and their influence on Antarctic lake ecosystems[J]. *Antarctic Research Series*, **59**, 53–70 (1993).
33. Salonen, K. *et al.* Perspectives in winter limnology: closing the annual cycle of freezing lakes[J]. *Aquat. Ecol*, **4** (3), 609–616 (2009).
34. James, P. & Terwilliger Salt rejection phenomena in the freezing of saline solutions[J]. *Research of Environmental Science*, **25** (8), 1331–1349 (1970).
35. Qin, X. *et al.* Chemical Characteristics of Waters in Rongbu Glacier on Mount Everest[J]. *Environmental Science*, **20** (001), 1–6 (1999).
36. Zhang, Y. *et al.* Total nitrogen migration in Ulansuhai Lake during ice growth process[J]. *Advances in Water Science*, **24** (005), 728–735 (2013).
37. Yu, T., Ma, J. & Li, Q. Factors affecting ice crystal purity during freeze concentration process for urine treatment[J]. *Journal of Harbin Institute of Technology*, **14** (05), 593–597 (2007).
38. Luo, C., Chen, W. & Han, W. Experimental study on factors affecting the quality of ice crystal during the freezing concentration for the brackish water[J]., **260** (1), 231–238 (2010).
39. Yu, T. & Ma, J. Study on influence of ice crystal purity during freeze concentration process[J]. *Journal of Harbin University of Commerce(Sciences Edition)*, **21** (05), 572–574578 (2005).
40. Tang Y, Zhang Y, Zhao W, et al. The migration law of iron during the process of water freezing[J]. *Water*, 2020, 12(2): 441.

Figures

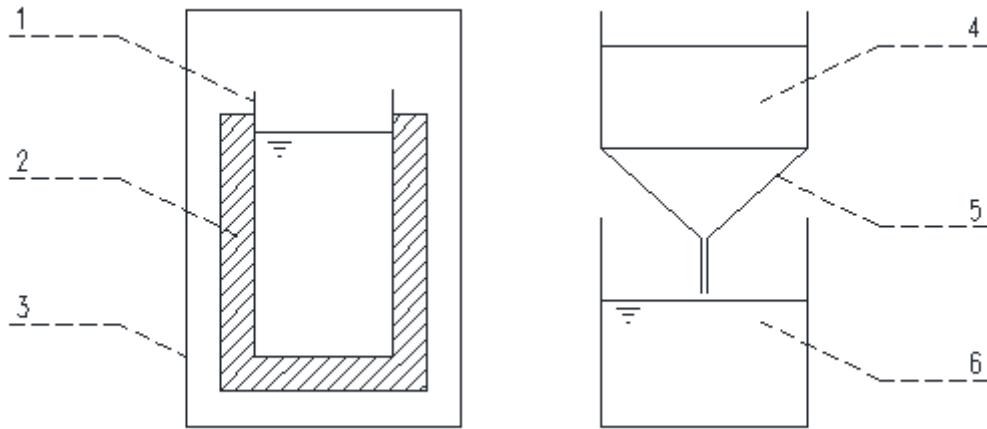


Figure 1

Ice formation device and ice melting device 1- cylindrical glass container; 2- polystyrene (EPS); 3- freezing simulation device; 4- ice sample; 5- funnel with glass mesh; 6- ice-melt water

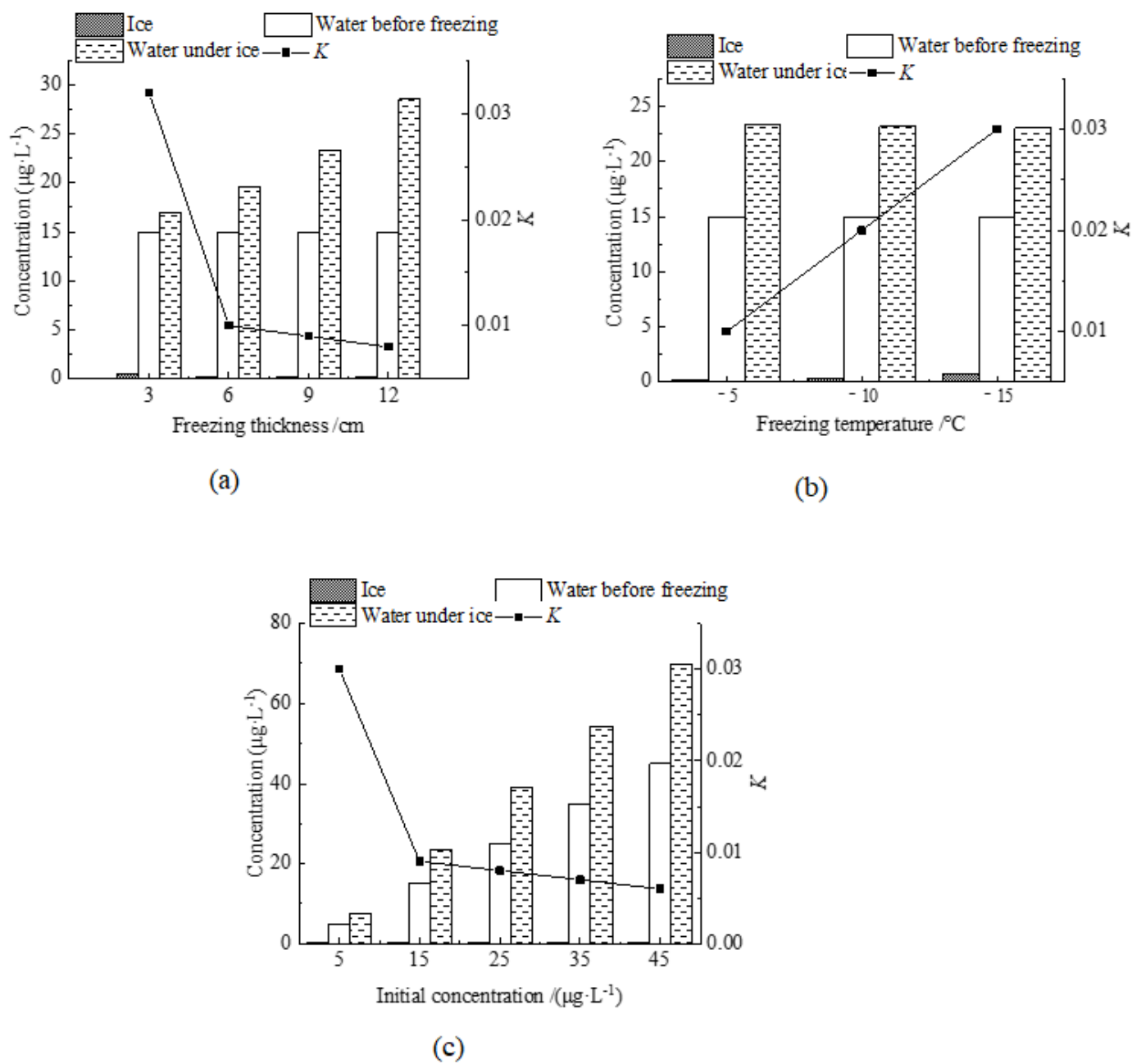


Figure 2

Distribution of atrazine in an ice–water system under different influencing factors (a) The influence of different ice thickness on the distribution of atrazine; (b) The influence of different freezing temperatures on the distribution of atrazine; (c) The influence of different initial concentrations on the distribution of atrazine

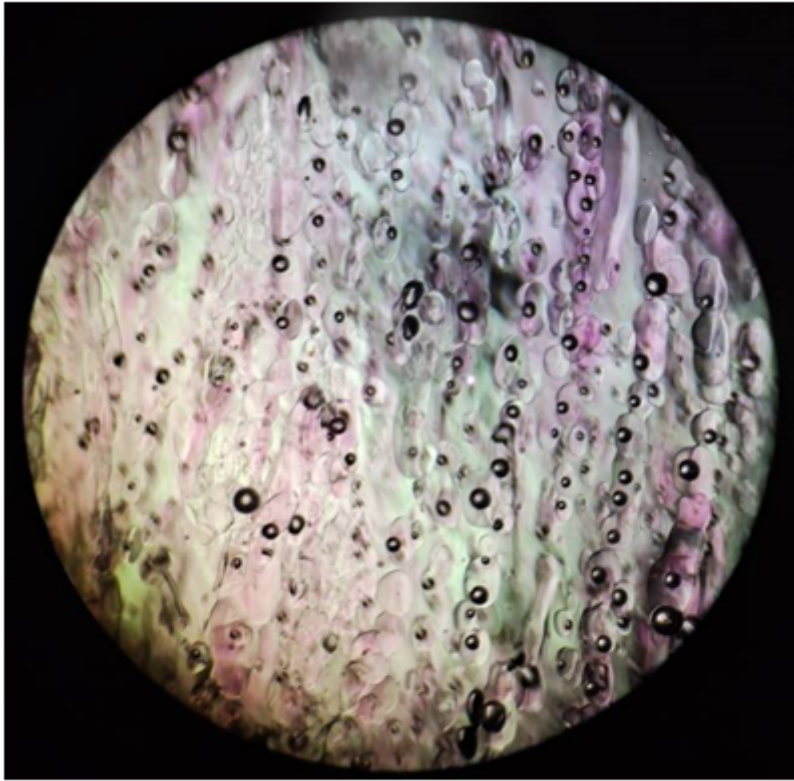


Figure 3

Schematic of ice structure cross section (KMnO4)

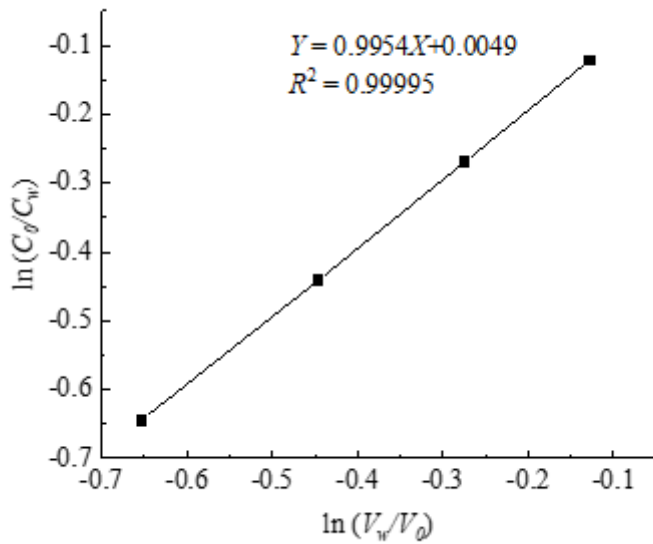


Figure 4

Relationship between V_w/V_0 and C_0/C_w during freezing of a $15 \mu\text{g}\cdot\text{L}^{-1}$ atrazine solution at -5°C